Supplement of Atmos. Chem. Phys., 23, 2003–2033, 2023
https://doi.org/10.5194/acp-23-2003-2023-supplement

Atmospheric Chemistry and Physics
Open Access

Supplement of

Experimental chemical budgets of OH, HO_2, and RO_2 radicals in rural air in western Germany during the JULIAC campaign 2019

Changmin Cho et al.

Correspondence to: Hendrik Fuchs (h.fuchs@fz-juelich.de) and Anna Novelli (a.novelli@fz-juelich.de)

Table S1. HO_2 and RO_2 background signals converted into apparent ambient concentrations used in the evaluation of HO_2 and RO_2 measurements. The average background signals originate from the reference experiments in the chamber while the upper limits are obtained from calibrations.

	HO_2 background 10^7 cm^{-3}	HO_2 background upper limit 10^7 cm^{-3}	RO_2 background 10^7 cm^{-3}	RO_2 background upper limit 10^7 cm^{-3}
Winter	0.4±0.6	1.2	0.5±0.2 2.8±0.4[a]	2.8
Spring	1.0±0.15	2.0	0.5±0.2	2.5
Summer	1.0±0.6	2.1	2.8±0.5	5.4
Autumn	0.0±0.4	1.5	0.0±0.4	1.5

[a] Variable background signals that are equivalent to RO_2 concentrations: from 14 Jan. to 25 Jan.: (0.5±0.2) × 10^7 cm^{-3}, from 26 Jan. to 6 Feb.: (1.6±0.2) × 10^7 cm^{-3}, from 07 Feb. to 10 Feb.: (2.8±0.4) × 10^7 cm^{-3}.

Table S2. List of the used VOCs for the radical budget analysis.

Classification	Species	Instrument
alkenes	pentene, hexene	VOCUS- PTR-TOF-MS
aromatics	toluene, xylene, benzene, phenol, furan, styrol, cresol	PTR-TOF-MS
BVOCs	isoprene, monoterpenes, sesquiterpenes	VOCUS- PTR-TOF-MS
OVOCs	acetaldehyde, acetone, acetonitrile, acrolein, adipinic acid, benzaldehyde, butanone, cyclohexanone, formic acid, glycolaldehyde, glycolic acid, hydroxyacetone, methylglyoxal, methyl vinyl ketone, methacrolein, nopinone, pentanone, pinonaldehyde, succinic acid	VOCUS- PTR-TOF-MS

Table S3. Meteorological and trace gas conditions during the specific period for Case 1 and 2.

	Case 1 (05.08 - 08.08.2019)		Case 2 (22.08 - 31.08.2019)	
Parameter	Median	Interquartile	Median	Interquartile
SAPHIR temperature (°C)	27.0	7.8	31.0	9.1
H_2O (%)	1.44	0.25	1.4	0.5
OH (10^6 cm^{-3})	4.5	5.2	4.1	5.7
HO_2 (10^8 cm^{-3})	1.4	1.4	2.7	3.8
RO_2 (10^8 cm^{-3})	2.1	2.6	2.9	3.1
O_3 (ppbv)	37.5	11.3	57.5	37.6
NO (ppbv)	0.26	0.39	0.22	0.54
NO_2 (ppbv)	3.4	2.2	4.3	4.6
CO (ppmv)	0.12	0.01	0.16	0.03
HCHO (ppbv)	1.8	0.7	3.4	1.8
HONO (ppbv)	0.18	0.09	0.21	0.15
k_{OH} (s^{-1})	5.2	1.1	8.7	3.4
k_{VOC} (s^{-1})	3.3	0.9	5.7	3.4
Total aerosol surface area (10^7 nm^2 cm^{-3})	8.5	2.5	11.2	11.7

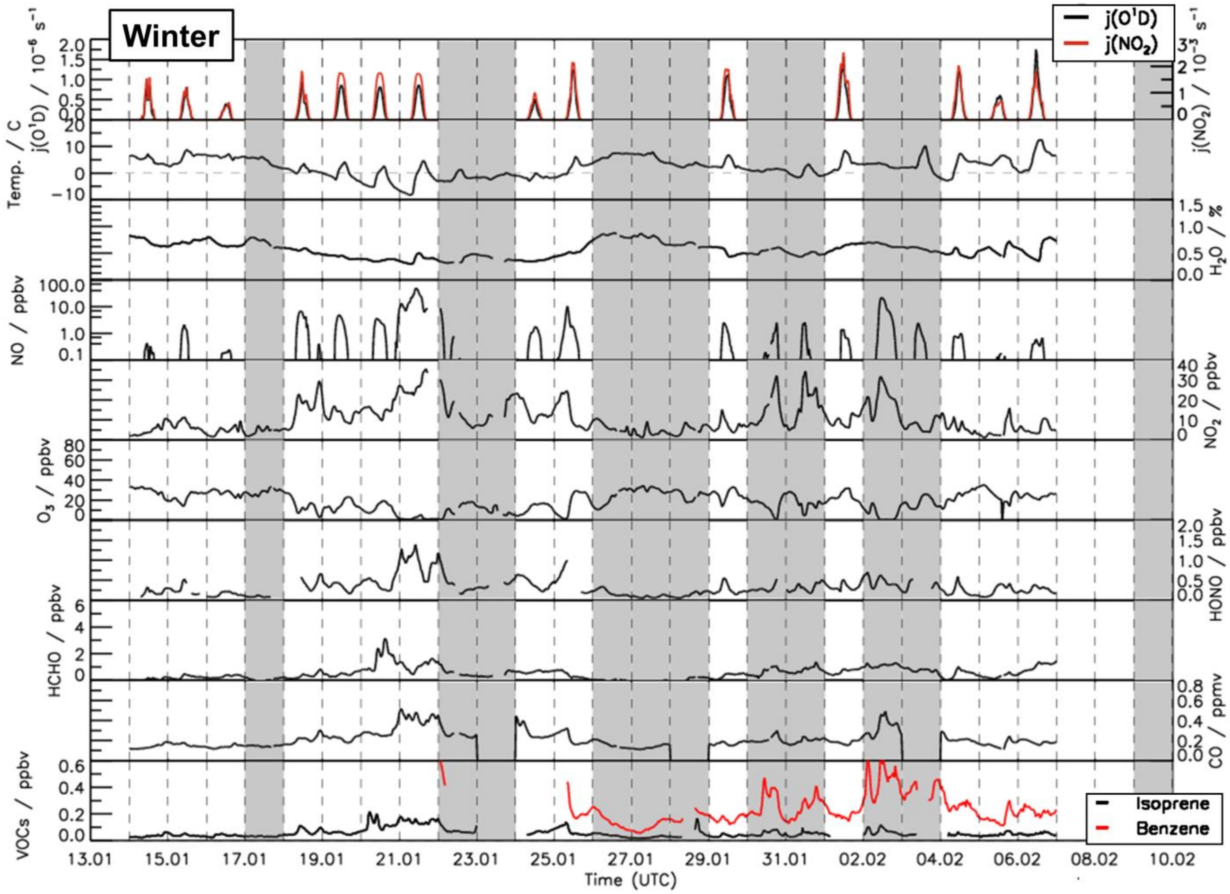

Figure S1: Time series of temperature and trace gas concentrations during the winter period of the JULIAC campaign (Cho et al., 2022). Vertical dashed lines denote midnight. Grey shaded areas indicate calibration days, when no measurements were done and days when the chamber roof was closed due to bad weather conditions.

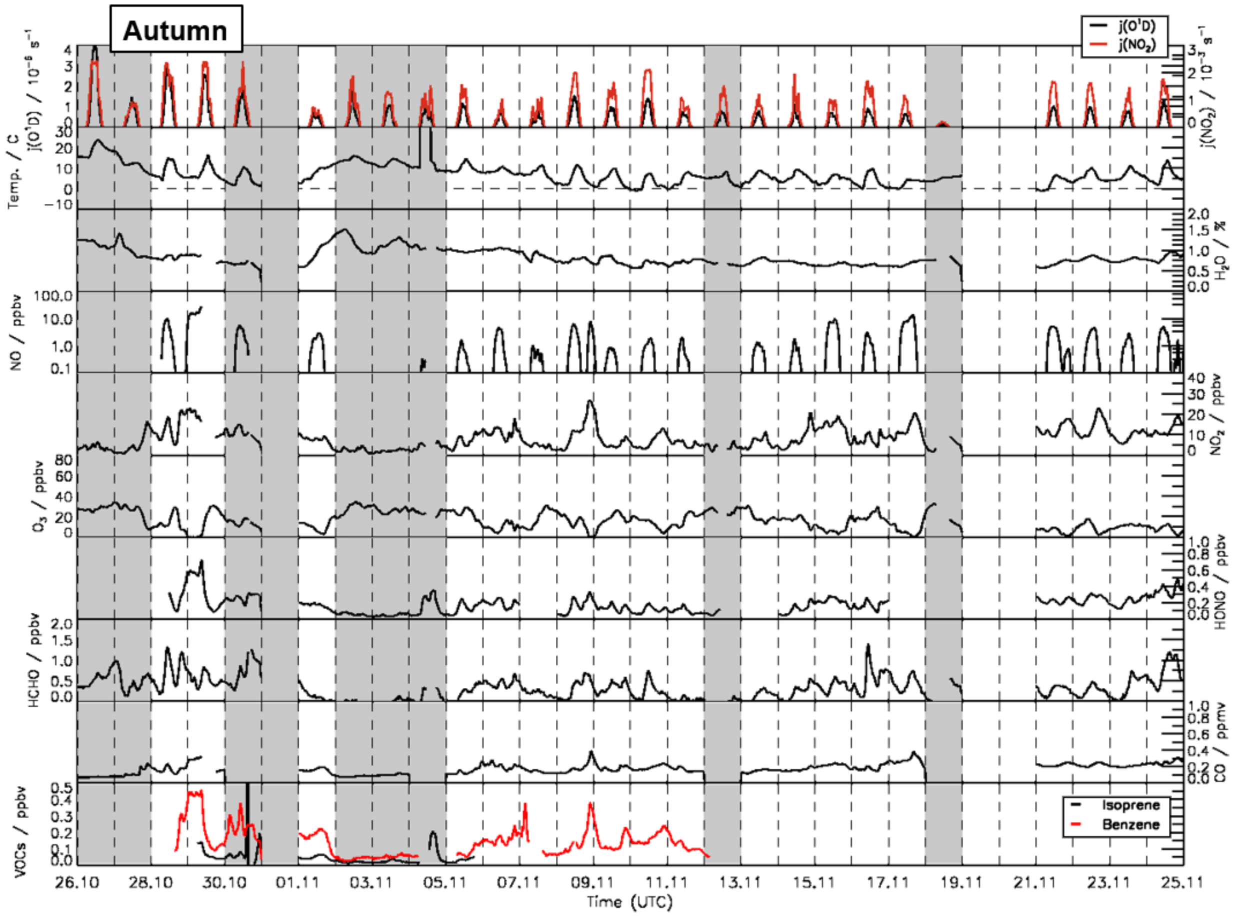

Figure S2: Time series of temperature and trace gas concentrations during the autumn period of the JULIAC campaign (Cho et al., 2022). Vertical dashed lines denote midnight. Grey shaded areas indicate calibration days, when no measurements were done and days when the chamber roof was closed due to bad weather conditions.

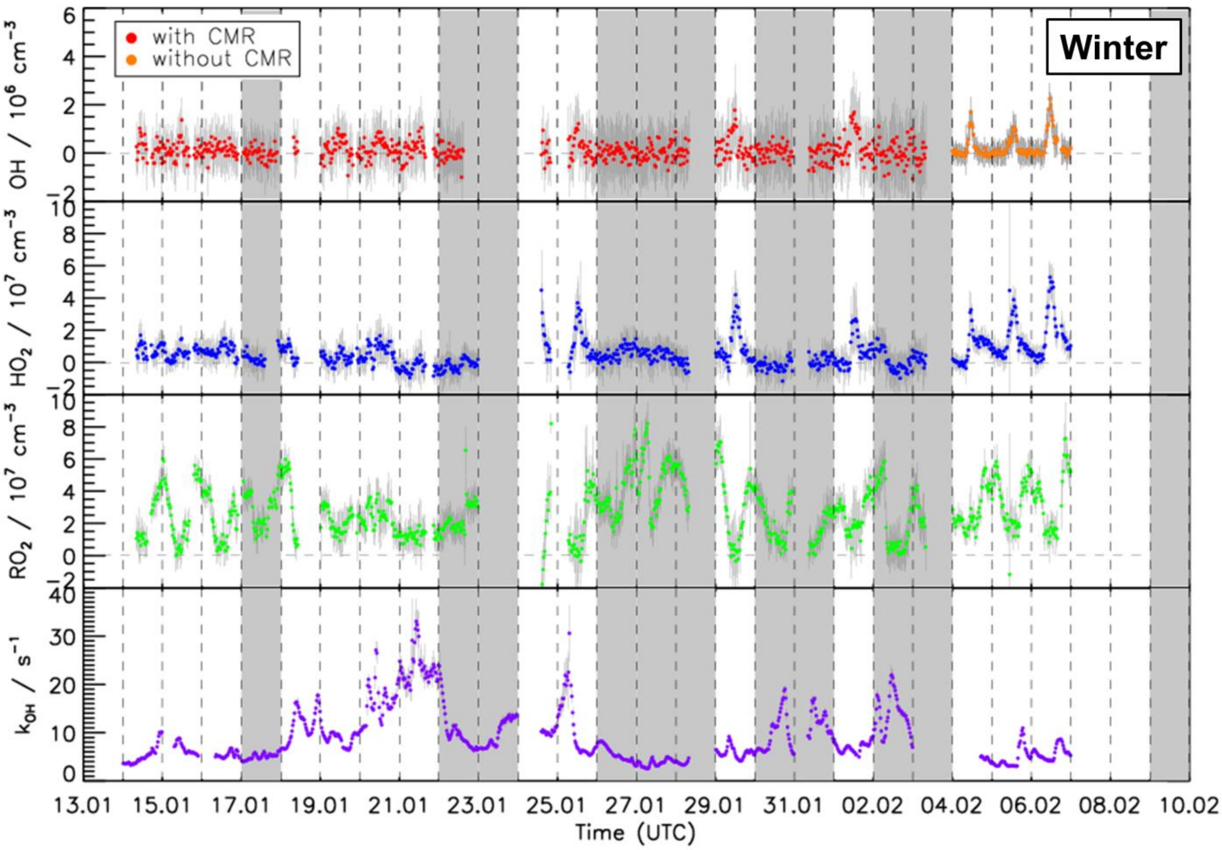

Figure S3: Time series of OH, HO_2, and RO_2 radical concentration measured by the FZJ-LIF-CMR instrument and measurements of the OH reactivity (k_{OH}) measured in the winter period of the JULIAC campaign (Cho et al., 2022). Vertical bars represent 1σ statistical errors. Vertical dashed lines denote midnight. Grey shaded areas indicate calibration days when no measurements were done and days when the chamber roof was closed due to bad weather conditions.

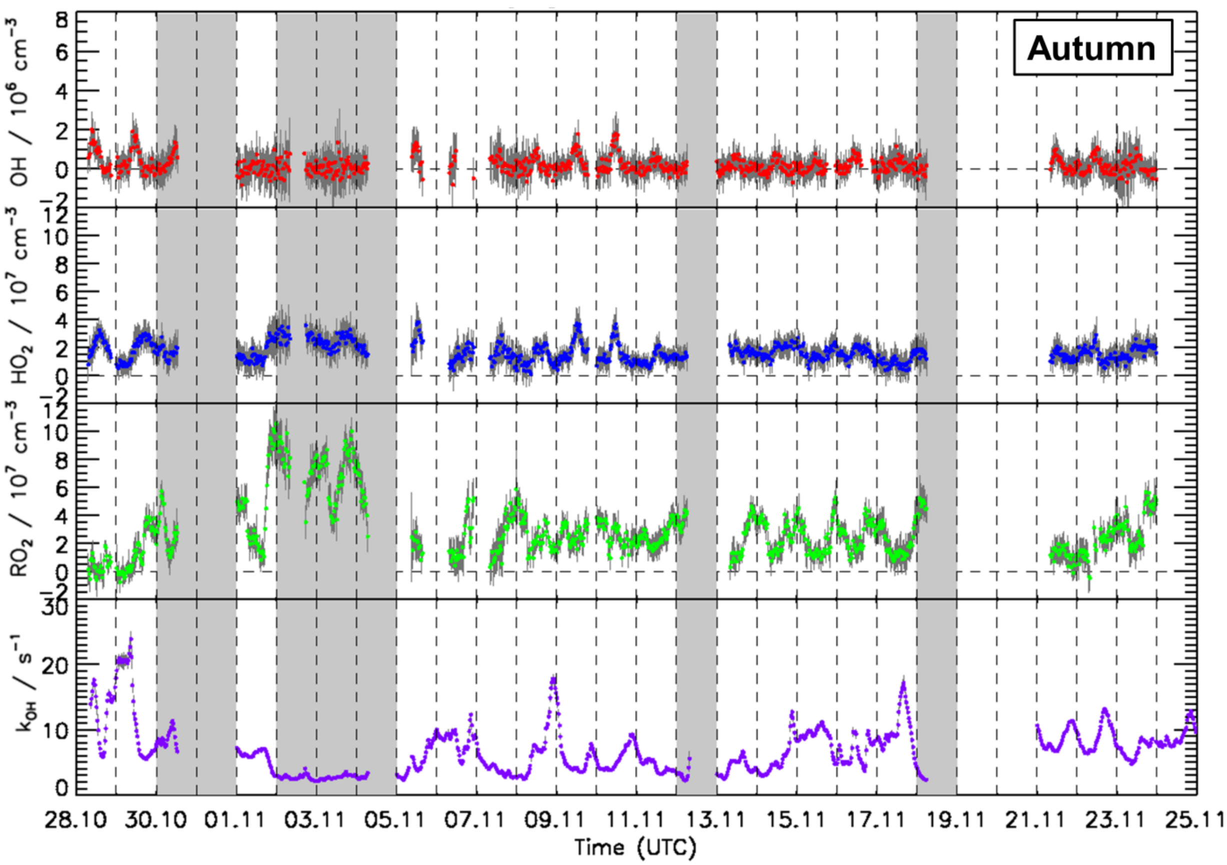

Figure S4: Time series of OH, HO_2, and RO_2 radical concentration measured by the FZJ-LIF-CMR instrument and measurements of the OH reactivity (k_{OH}) measured in the autumn period of the JULIAC campaign (Cho et al., 2022). Vertical bars represent 1σ statistical errors. Vertical dashed lines denote midnight. Grey shaded areas indicate calibration days when no measurements were done and days when the chamber roof was closed due to bad weather conditions.

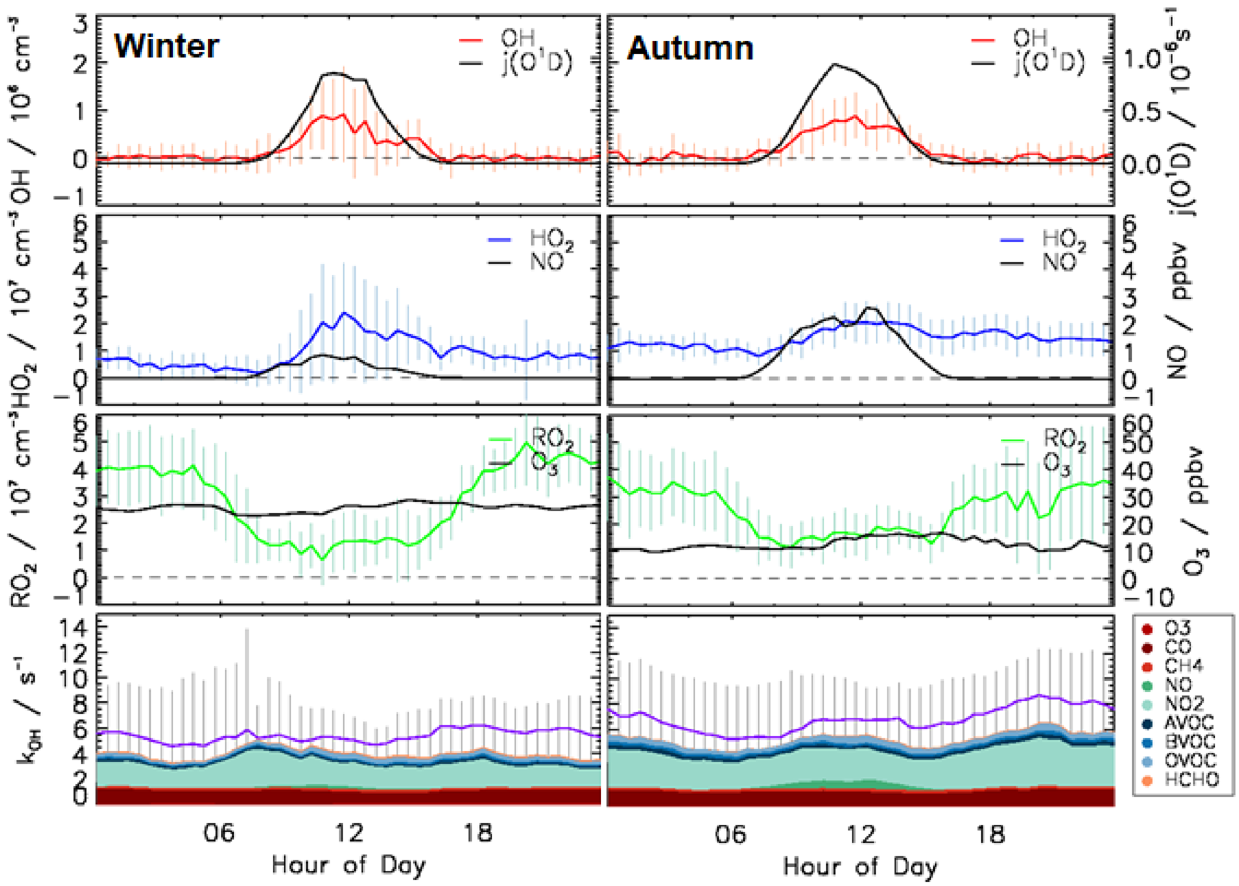

Figure S5: Median values of the diurnal profiles of OH, HO_2, RO_2, k_{OH}, j_{O1D}, NO, O_3 measured in the winter and autumn periods of the JULIAC campaign. Colored areas represent the contributions of measured reactants to the total OH reactivity. Vertical lines give 25th and 75th percentile values.

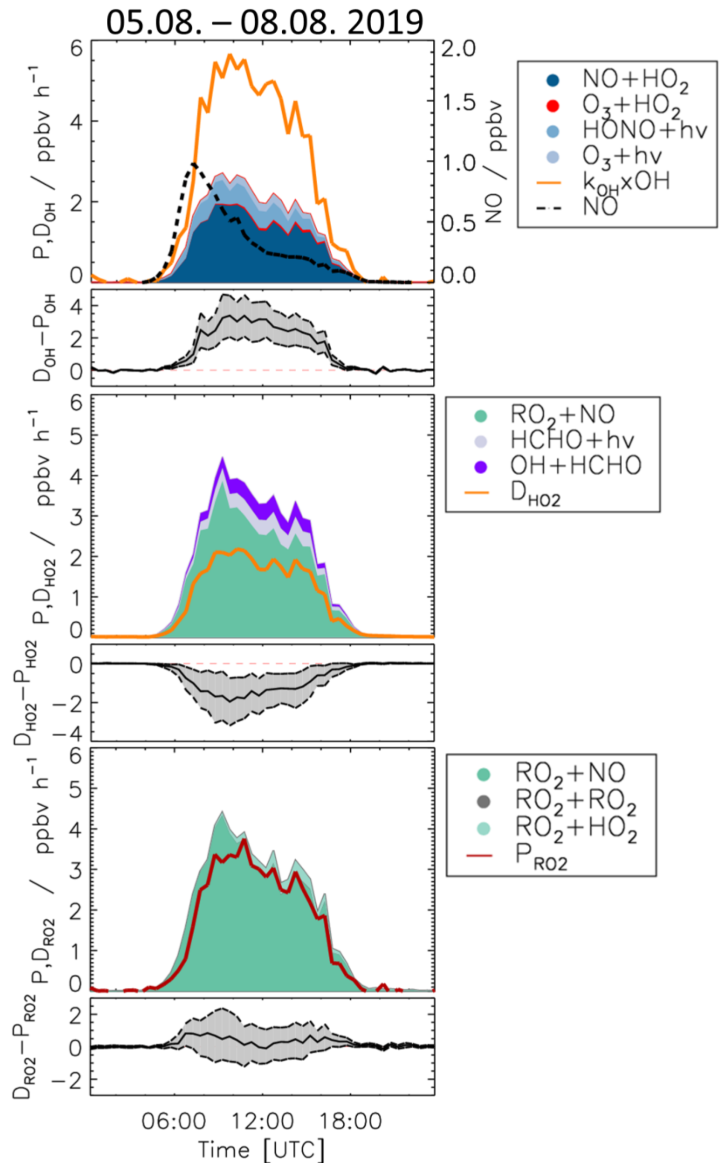

Figure S6: Chemical budgets for OH, HO_2, and RO_2 radicals similar to Figure 12 (only Case 1), using the lower limit of the reaction rate coefficient of the reaction of RO_2 with NO, $\mathbf{7.7 \times 10^{-12}}$ cm^3 s^{-1} (at 298 K for CH_3O_2) to calculate the turnover rate of this reaction. Grey areas indicate the 1σ uncertainty derived from experimental errors of the measured quantities (Table 2) and of the reaction rate constants (Table 1).

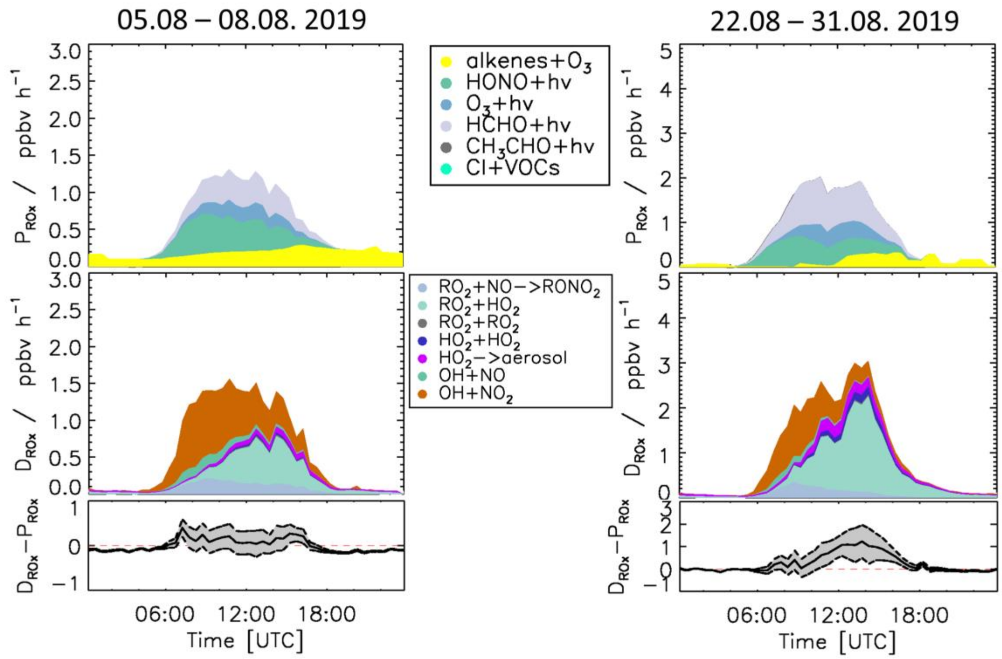

Figure S7: Experimental budgets for RO_X similar to Figure 11 (Case 1 and 2), using the high limits of alkene concentrations contributing to radical production by ozonolysis reactions and applying the HO_2 uptake on the aerosols (Section 4.2). Grey areas indicate the 1σ uncertainty derived from experimental errors of the measured quantities (Table 2) and of the reaction rate constants (Table 1).